Title

Generation of Functional Thymic Epithelium from Human Embryonic Stem Cells that Supports Host T Cell Development

Journal

Cell Stem Cell, 13(2)

ISSN

1934-5909

Authors

Parent, Audrey V
Russ, Holger A
Khan, Imran S
et al.

Publication Date

2013-08-01

DOI

10.1016/j.stem.2013.04.004

Peer reviewed

Published in final edited form as:
Cell Stem Cell. 2013 August 1; 13(2): . doi:10.1016/j.stem.2013.04.004.

Generation of Functional Thymic Epithelium from Human Embryonic Stem Cells that Supports Host T Cell Development

Audrey V. Parent[1], **Holger A. Russ**[1], **Imran S. Khan**[1], **Taylor N. LaFlam**[1], **Todd C. Metzger**[1], **Mark S. Anderson**[1,2,*], and **Matthias Hebrok**[1,2,*]

[1]Diabetes Center, Department of Medicine, University of California, San Francisco, San Francisco, CA 94143-0540, USA

SUMMARY

Inducing immune tolerance to prevent rejection is a key step toward successful engraftment of stem-cell-derived tissue in a clinical setting. Using human pluripotent stem cells to generate thymic epithelial cells (TECs) capable of supporting T cell development represents a promising approach to reach this goal; however, progress toward generating functional TECs has been limited. Here, we describe a robust in vitro method to direct differentiation of human embryonic stem cells (hESCs) into thymic epithelial progenitors (TEPs) by precise regulation of TGFβ, BMP4, RA, Wnt, Shh, and FGF signaling. The hESC-derived TEPs further mature into functional TECs that support T cell development upon transplantation into thymus-deficient mice. Importantly, the engrafted TEPs produce T cells capable of in vitro proliferation as well as in vivo immune responses. Thus, hESC-derived TEP grafts may have broad applications for enhancing engraftment in cell-based therapies as well as restoring age-and stress-related thymic decline.

INTRODUCTION

The use of stem cells to replace lost or damaged tissue represents one of the most promising applications of stem cell research. Among the most interesting and clinically relevant cell types that still haven't been successfully generated from human pluripotent stem cells are thymic epithelial cells (TECs). The thymus plays a crucial role in the immune system by supporting the development of functional T cells. It is also the main organ involved in establishing immune tolerance through the elimination of autoreactive T cell subsets (reviewed in Anderson et al., 2007). Both of these critical functions are mediated by TECs, the main component of the thymic stroma. Because the thymus undergoes profound degeneration with age and when exposed to stresses such as irradiation and chemotherapy, the use of stem cells as a potential source of TECs to enhance or restore thymic function is of great therapeutic interest. Given the key role of TECs in establishing self-tolerance, differentiation of a functional thymus from stem cells also has the potential to enhance engraftment of human-stem-cell-derived tissue through the induction of graft-specific immune tolerance. However, directed differentiation of human pluripotent stem cells into TECs has not been successful to date and remains an important challenge that needs to be addressed before such approaches can be developed.

*Correspondence: manderson@diabetes.ucsf.edu (M.S.A.), mhebrok@diabetes.ucsf.edu (M.H.).
[2]These authors contributed equally to the work

SUPPLEMENTAL INFORMATION

Supplemental Information for this article includes Supplemental Experimental Procedures and two figures and can be found with this article online at http://dx.doi.org/10.1016/j.stem.2013.04.004.

During embryogenesis, the thymus arises from the endoderm of the third pharyngeal pouch, a specialized pocket of the anterior foregut tube that contains the common primordium for the prospective thymus and parathyroid glands (Le Douarin and Jotereau, 1975; Gordon et al., 2004). The outgrowth of thymic epithelium occurs from the ventral domain of the third pharyngeal pouch in response to developmental cues such as FGFs, BMP4, and Wnt ligands (Balciunaite et al., 2002; Bleul and Boehm, 2005; Patel et al., 2006). Crosstalk with lymphoid progenitors that colonize the thymus subsequently allows differentiation of common thymic epithelial progenitors (TEPs) into two populations of mature TECs: cortical TECs (cTECs) and medullary TECs (mTECs) (Rodewald, 2008).

Although previous studies have reported the successful differentiation of human pluripotent stem cells into definitive endoderm (DE) and anterior foregut endoderm (AFE) (D'Amour et al., 2005; Green et al., 2011), they failed to demonstrate subsequent specification to the thymic lineage. Here we show that in-vitro-directed differentiation of human embryonic stem cells (hESCs) into TEPs can be achieved through recapitulation of the embryonic signaling events that guide thymic development in vivo. We have found that a precise temporal control of the activities of TGFβ, retinoic acid (RA), BMP, Wnt, Sonic Hedgehog (Shh), and FGF signaling is required to efficiently generate TEPs in vitro. Importantly, we demonstrate that TEPs derived using this method mature into functional TECs that support T cell development upon transplantation into athymic mice.

RESULTS

In-Vitro-Directed Differentiation of hESCs into TEPs

Even though the molecular mechanisms responsible for specifying thymus fate are still uncertain, prior work has identified the Foxn1 and Hoxa3 transcription factors as early and essential regulators of thymus specification and differentiation of TEPs into mature TECs (Manley and Capecchi, 1995; Nehls et al., 1996). We therefore focused our efforts on developing a stepwise protocol that recapitulates thymus organogenesis by using FOXN1 and HOXA3 expression as readouts for thymic specification.

As summarized in Figure 1A, hESCs were sequentially differentiated into DE, AFE, ventral pharyngeal endoderm (VPE), and TEPs. We first used a previously described method to induce differentiation into DE using activin A (D'Amour et al., 2005). At the end of stage 1, the majority of the cells coexpressed SOX17 and FOXA2, confirming efficient specification to DE (Figure S1A available online). Next, to promote the development of anteriorized and ventralized endoderm competent to give rise to $FOXN1^{+}HOXA3^{+}$ TEPs, we added activators and inhibitors of signaling pathways that have been shown to influence anterior-posterior and ventral-dorsal identities of emerging definitive endoderm (Zorn and Wells, 2009). We found that treatment of hESCs with high levels of activin A for 5 days (stage 1), followed by the addition of BMP4, RA, and the TGFβ inhibitor LY364947 (stage 2 and 3), and then BMP4 and RA alone (stage 4), led to a significant increase in *FOXN1* and *HOXA3* expression over undifferentiated hESCs at the end of stage 4 (Figure 1B, condition 6). In addition, hESCs differentiated under these conditions expressed *EYA1* and *GCM2*, two markers found in the developing third pharyngeal pouch (Figure S1B), thus con-firming the formation of pharyngeal endoderm (PE) in our cultures. Interestingly, *HOXA3* and *EYA1* expression levels obtained with these culture conditions were not as high as those observed with other treatments (Figures 1B and S1B, conditions 1–5). These observations suggest that specification to the thymic lineage occurs more efficiently when the levels of expression of these key factors remain below a certain threshold. Importantly, our results also reveal that the duration of the activin A treatment, as well as the presence of BMP4 and RA during stages 2–4, are crucial to induce high levels of *FOXN1* expression (Figure 1B, conditions 2–6).

Next, to optimize the efficiency of differentiation of AFE to VPE and TEPs, cells were differentiated up to stage 2 with condition 6 before being exposed to additional molecules involved in pharyngeal pouch patterning or involved directly in the induction of Foxn1 expression (Balciunaite et al., 2002; Frank et al., 2002; Bleul and Boehm, 2005; Moore-Scott and Manley, 2005; Gordon et al., 2010; Neves et al., 2012). We found that the simultaneous addition of BMP4, RA, Wnt3a, FGF8b, and the Shh inhibitor cyclopamine at stages 3 and 4 led to an even more robust induction of *FOXN1*, while maintaining levels of *HOXA3* and *EYA1* similar to those found in human fetal thymus (Figures 1B and S1B, condition 7). Immunostaining and flow cytometry analysis of cultures at the end of stage 4 confirmed that a significant number of cells differentiated under these conditions expressed HOXA3 (13.7% ± 2.8%) and EpCAM (95% ± 2%), an epithelial marker expressed by many epithelial cells, including TEPs (Rossi et al., 2006) (Figures 1C and S1C). Taking into account that the optimized protocol (condition 7) typically generated 1,000,000 cells from a starting population of 1,000,000 undifferentiated hESCs, this method thus yielded approximately 14% $HOXA3^{+}EpCAM^{+}$ double-positive output cells. Additional gene expression analysis for markers of other endoderm derivatives revealed that, while markers of thyroid (*NKX2.1*, *PAX8*), lung (*NKX2.1*, *FOXP2*), parathyroid (*PTH*), and pancreas (*PDX1*) were not expressed, low levels of liver markers (*AAT*, *ALB*, *CYP3A4*, and *CYP3A7*) could be detected (Figure S1D), suggesting that some cells were specified to the liver lineage. Given that *FOXN1* is also expressed in skin epithelial cells, we further tested for the presence of markers of early skin differentiation (*KRT1* and *KRT10*). The absence of such markers (Figure S1D) rules out the possibility that the induction in *FOXN1* expression was due to the generation of ectoderm-derived skin cells in the cultures. The optimized differentiation protocol was also tested on HUES4 cells to assess efficiency in another hESC line. As shown in Figures S1E–S1G, *FOXN1* and *HOXA3* mRNA transcription, as well as HOXA3 and EpCAM protein expression, were significantly induced. These data indicate that the differentiation protocol can be applied to other pluripotent stem cell lines. Taken together, these results demonstrate that efficient commitment of hESCs to the thymic lineage can be attained by precisely regulating the activities of TGFβ, BMP4, RA, Wnt, Shh, and FGF signaling throughout differentiation.

hESC-Derived TEPs Mature into TECs In Vivo

Although differentiated cells in our cultures express genes important for thymic identity such as *FOXN1*, *HOXA3*, and *EYA1*, marker genes characteristic of mature TECs such as *HLA-DRA* (MHC class II molecule) and *AIRE* were not detected (data not shown). This was not surprising since interactions of TEPs with developing T cell progenitors are necessary to stimulate maturation into functional TECs (Shores et al., 1994; Holländer et al., 1995; Klug et al., 2002). To test the capacity of in vitro generated TEPs to further mature, we transferred them to an environment where they would be in contact with lymphoid progenitors. We employed nude mice carrying a mutation in *Foxn1* that prevents the development of a functional thymus without precluding the formation of a lymphoid progenitor compartment. hESC-derived TEPs were thus transplanted under the kidney capsule of nude mice and grafts were analyzed 8–20 weeks later for the expression of genes found in mature TECs. Nude mice grafted with human fetal thymus (HFT) were used as positive controls. As shown in Figure 2A, while *FOXN1* was expressed at similar levels in grafts when compared to in vitro differentiated TEPs, a substantial upregulation in the expression of the differentiated TEC marker genes *HLA-DRA*, Delta-like 4 (*DLL4*), *CCL25*, *CXCL12*, and *SCF* was observed in TEP grafts, indicating increased maturation of TEPs upon transplantation. Expression of *AIRE* was not detected in TEP grafts (data not shown). Immunofluorescence analysis using an antibody recognizing a wide spectrum of different cytokeratins demonstrated the presence of epithelial structures in the grafts (Figure 2B). More importantly, antibodies for cytokeratins marking mature mTECs (K5) and cTECs (K8)

revealed $K5^+$ and $K8^+$ areas resembling normal thymic architecture in the TEP grafts, similar to that observed in HFT grafts (Figure 2C). These results suggest that $K5^+K8^+$ TEPs in hESC-derived grafts can give rise to $K5^+K8^-$ and $K5^-K8^+$ TECs in vivo. Taken together, these data indicate that hESC-derived TEPs acquire characteristics of mature TECs upon transplantation into athymic nude mice.

hESC-Derived TECs Support the Development of New T Cells

In addition to providing an appropriate environment for the maturation of TEPs into TECs, this experimental system also allows for testing of the functionality of transplanted cells. Indeed, when provided with functional thymic tissue from mouse (Gordon et al., 2004; Bleul et al., 2006) or human (Kollmann et al., 1993) origin, the lymphoid progenitors of nude mice can develop into mature T cells through the typical stepwise progression of $CD4^-CD8^-$ double-negative (DN), $CD4^+CD8^+$ double-positive (DP), and mature single-positive (SP) $CD4^+$ or $CD8^+$ T cells. To assess the functionality of transplanted TEPs generated using our method, we monitored the emergence of DP and SP T cells in the peripheral blood, secondary lymphoid organs, and grafts. Mice grafted with either hESCs differentiated with a control protocol (spontaneous hESCs differentiation in the absence of signaling factors) or HFT served as negative and positive controls, respectively.

As reported previously, a small number of extrathymically generated $CD4^+$ and $CD8^+$ SP T cells were detected in the peripheral blood and spleens of nongrafted and control-grafted nude mice (Figure 3A and Figure 4A) (Kennedy et al., 1992; Bleul et al., 2006). However, starting approximately 10 weeks after transplantation, we observed an increase in the number of $CD4^+$ and $CD8^+$ SP T cells specifically in the peripheral blood of TEP and HFT recipient mice (Figure 3A), suggesting that transplanted TEPs could support the generation of new T cells. Consistent with this result, histological analysis of hematoxylineosin (H&E) stained tissue revealed the presence of lymphoid cells in the grafts (Figure S2A). Immunofluorescence and flow cytometry analysis of grafts harvested 4–12 weeks (for HFT) or 8–25 weeks (for TEP and control) after transplantation demonstrated that $CD4^+CD8^+$ DP T cells, as well as $CD4^+$ and $CD8^+$ SP T cells, could be detected in TEP and HFT grafts, but not in control grafts (Figures 3B–3D and S2B–S2C). Although the total number of T cells isolated from HFT and TEP grafts was lower than what is normally found in thymopoietic tissue (Figure S2D), there were no significant differences between the two groups. These results confirmed that hESC-derived TEPs could indeed support thymopoiesis upon transplantation into athymic mice. Notably, similar to what is observed during the progression from DP to SP T cells in a normal mouse thymus, the T cell receptor (TCR) complex proteins CD3 and TCRβ were properly expressed on DP and SP T cells from TEP and HFT grafts (Figure 3E), indicating successful T cell receptor gene rearrangement and positive selection of newly generated T cells. While we saw clear evidence for canonical T cell maturation, we also observed variations in the kinetics and extent of thymopoiesis between TEP-grafted and HFT-grafted mice and between mice of the same group (Figures 3A–3D and S2A–S2C). A likely explanation comes from the differences in the developmental stage of TECs in HFT grafts when compared to hESC-derived TEPs, as well as from variations in engraftment efficiency. Thymopoiesis was also not sustained over prolonged periods of time as revealed by the progressive decline in the number of DP T cells in both TEP grafts and HFT grafts (Figure S2B). Since nude mice possess residual natural killer cell activity and can also develop autoimmunity in multiple organs following xenogeneic transplantation of thymic tissue (Taguchi et al., 1986; Fudaba et al., 2008), it is possible that the grafts are being damaged over time, leading to a decrease in thymopoiesis. Immunofluorescence analysis of HFT and TEP grafts for the mitotic marker Ki67 also showed that, while low levels of proliferating $cytokeratin^+$ cells could be detected in HFT and TEP grafts (Figure S2E), most $CD3^+$ T cells were found to be negative for Ki67 (Figure

S2F). Taken together, the increase in $CD4^+$ and $CD8^+$ SP T cells in the peripheral blood of TEP-grafted mice combined with the presence of $CD4^+CD8^+$ DP and SP T cells in the grafts clearly demonstrate that hESC-derived TEPs can support the development of new T cells.

T Cells Generated in TEP-Recipient Nude Mice Are Functional

In addition to the T cells detected in the grafts, we also found evidence of migration of functional T cells to the peripheral immune system in TEP-grafted mice. As shown in Figures 4A and 4B, a significant increase in $CD4^+$ and $CD8^+$ SP T cell populations, and more prominently, in $TCR\beta^+CD4^+$ and $TCR\beta^+CD8^+$ T cells, could be detected in the spleen of HFT and TEP-grafted mice over nongrafted and control-grafted mice. Importantly, we also observed positive selection of $CD4^+Foxp3^+$ regulatory T cells (Tregs), a subset of lymphocytes essential for establishing immune tolerance through suppression of autoreactive T cells (Sakaguchi, 2000). In HFT and TEP-grafted mice, 4.6% ± 1.8% and 2.9% ± 0.8% of total $CD4^+$ cells were positive for Foxp3, whereas only 0.4% ± 0.3% and 0.2% ± 0.1% were positive in control and nongrafted mice, respectively (Figure 4C). Thus, not only did we observe increased formation of T cells, hESC-derived TEPs also promoted formation of T cell subsets otherwise almost completely absent in control animals.

Furthermore, spectratype analysis of the TCR repertoire of cells recovered from nude recipient mice indicated more diverse TCR Vβ rearrangements in HFT and TEP recipients in comparison to control mice (Figures 4D and 4E), demonstrating that hESC-derived TECs can support the development of T cells with a diverse TCR repertoire. Another critical test for T cell function is their ability to proliferate upon TCR stimulation. Labeling of cells with carboxyfluorescein diacetate succinimidyl ester (CFSE) followed by stimulation with anti-CD3/CD28 antibodies revealed that 74% ± 6% of $CD4^+$ and 84% ± 6% of $CD8^+$ T cells isolated from HFT-grafted mice and 47% ± 3% of $CD4^+$ and 68% ± 5% of $CD8^+$ T cells isolated from TEP-grafted mice proliferated following TCR stimulation (Figure 5A). These results indicate that a significant portion of newly formed T cells is functional and responsive to activation signals through the TCR. Relative to wild-type (WT) mice, lower TCR diversity and lower levels of TCR stimulation-induced proliferation were seen in HFT- and TEP-grafted mice (Figure 4E and Figure 5A), consistent with cross-species differences that likely impair full activation/differentiation of murine T cells upon interaction with human TECs (Taguchi et al., 1986; Kollmann et al., 1993; Fudaba et al., 2008). In addition, significant proliferation of T cells from HFT-grafted mice and $CD8^+$ T cells from TEP-grafted mice was observed in response to allogeneic stimulator cells (Figure 5B), indicating that T cells are capable of allogeneic responses. $CD4^+$ T cells from HFT-grafted mice and $CD8^+$ T cells from TEP-grafted mice also proliferated in response to stimulator cells from nu/+ mice (Figure 5C). This result supports the idea that T cells in HFT- and TEP-grafted mice have been selected on human MHC and are thus responding to MHC-mismatched stimulator cells. As an additional measure of functionality, we evaluated the ability of grafted mice to reject allogeneic skin transplants. As shown in Figure 6, we observed increased graft rejection in HFT (median survival time or MST = 20.5 days) and TEP (MST = 19.5 days) recipient nude mice when compared with control mice (MST > 35 days), confirming that the T cells generated in HFT- and TEP-grafted mice are functional in vivo. Summarily, these data demonstrate the ability of transplanted TEPs to support the generation of new functional T cells in athymic nude mice.

DISCUSSION

Although many cell lineages generated from human pluripotent stem cells express appropriate marker genes, very few have been shown to give rise to fully differentiated functional cells. In this study, we present a method to differentiate hESCs into TEPs that mature into functional TECs when transplanted in vivo (Figure 7). Our study demonstrates

that the success of coaxing hESCs into functional TEPs depends on the accurate in vitro recapitulation of in vivo embryonic signaling events, including early specification of anterior-posterior and dorsal-ventral cell identities that are permissive for complete thymus development. Although it has been reported previously that anteriorization of DE can be achieved by blocking TGFβ signaling either alone (Mou et al., 2012) or in conjugation with BMP inhibition (Green et al., 2011; Longmire et al., 2012), we show that activation of RA signaling is also required for accurate anterior-posterior patterning of the foregut prior to thymic specification. Indeed, expression of the transcription factor HOXA3, a member of the Hox family that specifies positional identity along the anterior-posterior axis in the developing embryo, was not induced in the absence of RA. Consistent with previous studies showing that Hoxa3 is essential for thymic specification in vivo (Manley and Capecchi, 1995), our results strongly suggest that in vitro specification of hESCs to the thymic lineage also requires culture conditions that induce appropriate levels of expression of this transcription factor. Even though significant induction of *FOXN1* expression was observed with this method, the levels of expression were lower than what is found in control thymic tissue. This is most likely due to the generation of heterogeneous cultures, as suggested by the quantification of $HOXA3^{+}EpCAM^{+}$ cells, which represent approximately 14% of the cells. Future studies will focus on defining conditions that enhance efficiency of differentiation to the thymic lineage as well as improving the purity of the cells by isolating them using cell surface markers yet to be identified.

Importantly, our data reveal that transplantation of in-vitro-generated TEPs in athymic mice leads to the upregulation of multiple genes critical for TEC function. Indeed, hESC-derived TECs expressed the chemokines/cytokines *CCL25*, *CXCL12*, and *SCF*, which are normally produced by TECs to attract hematopoietic progenitors to the thymus and promote lymphoid progenitor development (Calderón and Boehm, 2012). In addition, hESC-derived TECs expressed Delta-like 4 (*DLL4*), a Notch ligand that induces the commitment of hematopoietic progenitors to the T cell lineage. The presence of this crucial molecule combined with the appropriate chemotactic cues thus most likely helped promote the homing and development of DP T cell progenitors in TEP grafts.

Furthermore, once T cell progenitors present in the thymus have rearranged the TCR gene and successfully progressed to the DP stage, their survival as well as their commitment to the $CD4^{+}$ or $CD8^{+}$ lineages depends on interaction with MHC-self-peptide complexes displayed on TECs. In addition to MHC class I molecules, which are expressed ubiquitously on most cells, the upregulation of MHC class II molecules by TEPs was likely to be critical for their ability to support positive selection of developing $CD4^{+}$ T cells. The capacity of hESC-derived TECs to successfully regulate the transition of DP to SP T cells was confirmed by the presence of an increased number of diverse and responsive SP T cells in the peripheral blood and spleen of TEP-grafted mice. However, even though a significant amount of $CD4^{+}$ SP T cells were generated in TEP-grafted mice, the efficiency was reduced when compared to HFT grafts, most likely due to lower MHC class II expression in hESC-derived TECs.

Importantly, T cells from TEP-grafted mice were responsive to direct TCR activation and stimulation by allogeneic antigen-presenting cells (APCs) in vitro. They could also mediate rejection of allogeneic skin grafts in vivo, further confirming their functionality. However, the response to allogeneic stimulator cells of $CD4^{+}$ T cells from TEP-grafted mice was lower than what was observed in WT and HFT mice, suggesting that this subset of T cells was not able to mount efficient responses against alloantigens. Further studies will be required to address this issue in more detail. Interestingly, TECs also promoted the generation of Tregs, a subset of T cells that are crucial for the maintenance of immune tolerance through the inhibition of self-reactive T cells in the periphery. Our data thus

clearly demonstrate that hESC-derived TEPs transplanted in athymic mice acquire characteristics of mature TECs that allow them to support multistage T cell development.

The ability to generate functional thymic epithelium from human pluripotent stem cells will have numerous applications, including enabling modeling of human immune diseases using patient-specific induced pluripotent stem cell (iPSC) lines. It will also make possible the use of stem cells as a potential source of TECs to enhance or restore thymic function. Importantly, since the thymus has the unique capacity to modify tolerance in an antigen-specific manner, transplantation of TEPs has the potential to promote graft-specific immune tolerance without the need for sustained immunosuppression (Nobori et al., 2006). By allowing the generation of a T cell repertoire tolerant to stem cell self antigens, cotransplantation of stem-cell-derived TECs could prevent immune rejection of other transplants derived from the same cell line, potentially having a major impact on the effectiveness of stem-cell-based therapies. This may be a particularly attractive approach in autoimmune disease settings such as type 1 diabetes, where both β cell replacement and immunomodulation are likely required for a successful outcome.

EXPERIMENTAL PROCEDURES

Cell Culture

Undifferentiated CyT49 and HUES4 hESCs were maintained on mitomycin-C-treated mouse embryonic fibroblast (MEF) feeders (Millipore) as previously described (D'Amour et al., 2006). For differentiation, hESCs were plated on MEFs at a density of 6.25×10^4 cells/cm^2 and differentiated 72 hr later as follows: stage 1 and 2 of differentiations were carried out in RPMI 1640 media (Invitrogen) supplemented with increasing concentrations of KSR (0% on day 1 [d1], 0.2% on d2–3, and 2% on d4) or B27 (0.5% on d5–7). For stages 3 and 4, cells were differentiated in DMEM/F12 with 0.5% B27. The following factors were added: activin A, 100 ng/ml (d1–5); Wnt3a, 25 ng/ml (d1) or 50 ng/ml (d8–11); all-trans retinoic acid (RA), 0.25 μM (d4–7) or 0.1 μM (d8–11); BMP4, 50 ng/ml (d6–11); LY364947, 5 μM (d6–9); FGF8b, 50 ng/ml (d8–11); and KAAD-cyclopamine, 0.5 μM (d8–11). Supplements and factors were from Invitrogen (B27, KSR), R&D Systems (activin A, Wnt3a, BMP4, and FGF8b), Sigma (RA), and Millipore (KAAD-cyclopamine, LY364947).

Real-Time Quantitative PCR

RNA extraction and real-time quantitative PCR from hESC cultures and dissected grafts was performed as described in the Supplemental Information.

Immunofluorescence

hESC cultures were fixed and immunostained according to the protocol described in the Supplemental Information. For tissue sections, kidneys were embedded in OCT medium (Tissue-Tek) and were processed as described in the Supplemental Information.

Kidney Capsule Implantations

hESC cultures differentiated using condition 1 (control) or 7 (TEP) were either incubated with Accutase for 5 min or cut into ~2–5 mm squares using a needle. Cell clumps were lifted with a cell scraper, collected by centrifugation, washed, and resuspended in differentiation media +10 μg/ml DNase I (Sigma). Following a 4–6 hr incubation at 37°C, ~$2–4 \times 10^6$ cells were implanted under the kidney capsule of nude mice as described (Russ and Efrat, 2011). HFT grafts were generated by implanting a ~1 mm^3 piece of HFT under the kidney capsule of nude mice using a similar technique. Fresh HFT was obtained from Advanced Bioscience Resources. Four to twenty-five weeks after transplantation, kidneys

were surgically extracted and the tissue was processed for histology, RNA extraction, or analysis by flow cytometry.

Flow Cytometry

Lymphocytes isolated by mashing thymi, dissected grafts, or spleens on a 40 μm cell-strainer were processed as described in the Supplemental Information.

Spectratyping

Total RNA was isolated from 5–10 × 10^6 splenocytes using TRIzol reagent (Invitrogen) and RNeasy Mini columns (QIAGEN) followed by reverse transcription into cDNA using SuperScript III first-strand synthesis system (Invitrogen). PCR and run-off reactions were performed using a common Cβ primer and primers specific for each TCR Vβ family as described previously (Currier and Robinson, 2001). Labeled products from the run-off reactions were analyzed using a 3130xl Genetic Analyzer (Applied Biosystems) and GeneMapper software (Applied Biosystems). The overall spectratype complexity score was determined as described in the Supplemental Information.

Proliferation Assay

Splenocytes (10^7) were labeled with a solution of 5 μm CFSE diluted in DMEM+2% FBS for 5 min at RT. An equal volume of FBS was added and cells were washed with DMEM +2% FBS. CFSE-labeled cells were then cultured in round-bottom 96-well plates precoated with anti-CD3 and anti-CD28 antibodies (10 μg/ml) at a cell density of 4 × 10^5 cells/well. After 3 days, loss of CFSE in $CD4^+$ and $CD8^+$ T cells was assayed by staining with anti-CD4 and anti-CD8 antibodies and analyzing by flow cytometry.

Mixed Lymphocyte Reaction

T cells and APCs were prepared as described in the Supplemental Information. CFSE-labeled T cells were added to round-bottom 96-well plates at 2 × 10^5 cells per well in complete DMEM media. Enriched dendritic cells were added to wells at 2 × 10^4 cells per well. After 4 days of culture, loss of CFSE in $CD4^+$ and $CD8^+$ T cells was assayed by staining with anti-CD90.2, anti-CD4, and anti-CD8 antibodies and analyzing by flow cytometry.

Skin Grafting

Ear skin from an allogeneic C57BL/6 donor mouse was placed on graft beds of approximately 8 mm^2 on the flanks of anesthetized recipient mice. Grafts were covered with Vaseline gauze and fixed with fabric strips. Bandages were removed 7 days later, and grafts were monitored every other day for signs of rejection. Grafts were considered rejected when >80% of the graft area was necrotic.

Mice

NU/J mice were obtained from Jackson Laboratories. Mice used in this study were maintained according to protocols approved by the UCSF Institutional Care and Use of Animals Committee (IACUC).

Statistics

Data was analyzed with GraphPad Prism software using an unpaired two-tailed Student's t test or a Mann-Whitney test. Error bars in bar diagrams represent standard deviation of the samples.

Supplementary Material

Refer to Web version on PubMed Central for supplementary material.

Acknowledgments

We thank members of the Anderson and Hebrok laboratories for helpful discussion. We thank Na Li, Kellsey Johannes, Debbie Ngow, and Jennifer Ringler for technical help; C. Stoddart and J. Rivera for help with kidney capsule transplantations; J. Puck and Y. Wang for help with analysis of the spectratyping data; Q. Tang and K. Lee for help with skin transplantations; and Viacyte for providing the CyT49 cell line. A.V.P. was supported by a Canadian Institutes of Health Research fellowship, H.A.R by a Richard G. Klein fellowship and JDRF fellowship (3-2012-266), and I.S.K. and T.N.L. by the UCSF Medical Scientist Training Program. Research in M.S.A.'s and M.H.'s laboratories was supported by a CIRM grant (CIRM RM1-01702). Imaging and flow cytometry experiments were supported by resources from the UCSF Diabetes and Endocrinology Research Center (DERC) and UCSF Flow Cytometry Core.

References

Anderson G, Lane PJL, Jenkinson EJ. Generating intrathymic microenvironments to establish T-cell tolerance. Nat Rev Immunol. 2007; 7:954–963. [PubMed: 17992179]

Balciunaite G, Keller MP, Balciunaite E, Piali L, Zuklys S, Mathieu YD, Gill J, Boyd R, Sussman DJ, Holländer GA. Wnt glycoproteins regulate the expression of FoxN1, the gene defective in nude mice. Nat Immunol. 2002; 3:1102–1108. [PubMed: 12379851]

Bleul CC, Boehm T. BMP signaling is required for normal thymus development. J Immunol. 2005; 175:5213–5221. [PubMed: 16210626]

Bleul CC, Corbeaux T, Reuter A, Fisch P, Mönting JS, Boehm T. Formation of a functional thymus initiated by a postnatal epithelial progenitor cell. Nature. 2006; 441:992–996. [PubMed: 16791198]

Calderón L, Boehm T. Synergistic, context-dependent, and hierarchical functions of epithelial components in thymic microenvironments. Cell. 2012; 149:159–172. [PubMed: 22464328]

Currier JR, Robinson MA. Spectratype/immunoscope analysis of the expressed TCR repertoire. Curr Protoc Immunol. 2001; Chapter 10(Unit 10.28)

D'Amour KA, Agulnick AD, Eliazer S, Kelly OG, Kroon E, Baetge EE. Efficient differentiation of human embryonic stem cells to definitive endoderm. Nat Biotechnol. 2005; 23:1534–1541. [PubMed: 16258519]

D'Amour KA, Bang AG, Eliazer S, Kelly OG, Agulnick AD, Smart NG, Moorman MA, Kroon E, Carpenter MK, Baetge EE. Production of pancreatic hormone-expressing endocrine cells from human embryonic stem cells. Nat Biotechnol. 2006; 24:1392–1401. [PubMed: 17053790]

Frank DU, Fotheringham LK, Brewer JA, Muglia LJ, Tristani-Firouzi M, Capecchi MR, Moon AM. An Fgf8 mouse mutant phenocopies human 22q11 deletion syndrome. Development. 2002; 129:4591–4603. [PubMed: 12223415]

Fudaba Y, Onoe T, Chittenden M, Shimizu A, Shaffer JM, Bronson R, Sykes M. Abnormal regulatory and effector T cell function predispose to autoimmunity following xenogeneic thymic transplantation. J Immunol. 2008; 181:7649–7659. [PubMed: 19017953]

Gordon J, Wilson VA, Blair NF, Sheridan J, Farley A, Wilson L, Manley NR, Blackburn CC. Functional evidence for a single endodermal origin for the thymic epithelium. Nat Immunol. 2004; 5:546–553. [PubMed: 15098031]

Gordon J, Patel SR, Mishina Y, Manley NR. Evidence for an early role for BMP4 signaling in thymus and parathyroid morphogenesis. Dev Biol. 2010; 339:141–154. [PubMed: 20043899]

Green MD, Chen A, Nostro MC, d'Souza SL, Schaniel C, Lemischka IR, Gouon-Evans V, Keller G, Snoeck HW. Generation of anterior foregut endoderm from human embryonic and induced pluripotent stem cells. Nat Biotechnol. 2011; 29:267–272. [PubMed: 21358635]

Holländer GA, Wang B, Nichogiannopoulou A, Platenburg PP, van Ewijk W, Burakoff SJ, Gutierrez-Ramos JC, Terhorst C. Developmental control point in induction of thymic cortex regulated by a sub-population of prothymocytes. Nature. 1995; 373:350–353. [PubMed: 7830770]

Kennedy JD, Pierce CW, Lake JP. Extrathymic T cell maturation. Phenotypic analysis of T cell subsets in nude mice as a function of age. J Immunol. 1992; 148:1620–1629. [PubMed: 1347303]

Klug DB, Carter C, Gimenez-Conti IB, Richie ER. Cutting edge: thymocyte-independent and thymocyte-dependent phases of epithelial patterning in the fetal thymus. J Immunol. 2002; 169:2842–2845. [PubMed: 12218095]

Kollmann TR, Goldstein MM, Goldstein H. The concurrent maturation of mouse and human thymocytes in human fetal thymus implanted in NIH-beige-nude-xid mice is associated with the reconstitution of the murine immune system. J Exp Med. 1993; 177:821–832. [PubMed: 8436912]

Le Douarin NM, Jotereau FV. Tracing of cells of the avian thymus through embryonic life in interspecific chimeras. J Exp Med. 1975; 142:17–40. [PubMed: 239088]

Longmire TA, Ikonomou L, Hawkins F, Christodoulou C, Cao Y, Jean JC, Kwok LW, Mou H, Rajagopal J, Shen SS, et al. Efficient derivation of purified lung and thyroid progenitors from embryonic stem cells. Cell Stem Cell. 2012; 10:398–411. [PubMed: 22482505]

Manley NR, Capecchi MR. The role of Hoxa-3 in mouse thymus and thyroid development. Development. 1995; 121:1989–2003. [PubMed: 7635047]

Moore-Scott BA, Manley NR. Differential expression of Sonic hedgehog along the anterior-posterior axis regulates patterning of pharyngeal pouch endoderm and pharyngeal endoderm-derived organs. Dev Biol. 2005; 278:323–335. [PubMed: 15680353]

Mou H, Zhao R, Sherwood R, Ahfeldt T, Lapey A, Wain J, Sicilian L, Izvolsky K, Musunuru K, Cowan C, Rajagopal J. Generation of multipotent lung and airway progenitors from mouse ESCs and patient-specific cystic fibrosis iPSCs. Cell Stem Cell. 2012; 10:385–397. [PubMed: 22482504]

Nehls M, Kyewski B, Messerle M, Waldschütz R, Schüddekopf K, Smith AJ, Boehm T. Two genetically separable steps in the differentiation of thymic epithelium. Science. 1996; 272:886–889. [PubMed: 8629026]

Neves H, Dupin E, Parreira L, Le Douarin NM. Modulation of Bmp4 signalling in the epithelial-mesenchymal interactions that take place in early thymus and parathyroid development in avian embryos. Dev Biol. 2012; 361:208–219. [PubMed: 22057081]

Nobori S, Shimizu A, Okumi M, Samelson-Jones E, Griesemer A, Hirakata A, Sachs DH, Yamada K. Thymic rejuvenation and the induction of tolerance by adult thymic grafts. Proc Natl Acad Sci USA. 2006; 103:19081–19086. [PubMed: 17148614]

Patel SR, Gordon J, Mahbub F, Blackburn CC, Manley NR. Bmp4 and Noggin expression during early thymus and parathyroid organogenesis. Gene Expr Patterns. 2006; 6:794–799. [PubMed: 16517216]

Rodewald HR. Thymus organogenesis. Annu Rev Immunol. 2008; 26:355–388. [PubMed: 18304000]

Rossi SW, Jenkinson WE, Anderson G, Jenkinson EJ. Clonal analysis reveals a common progenitor for thymic cortical and medullary epithelium. Nature. 2006; 441:988–991. [PubMed: 16791197]

Russ, HA.; Efrat, S. In-vivo functional assessment of engineered human insulin-producing cells. In: Soto-Gutierrez, A.; Kobayashi, N.; Fox, IJ., editors. Cell Transplantation. Norwood, MA: Artech House; 2011.

Sakaguchi S. Regulatory T cells: key controllers of immunologic self-tolerance. Cell. 2000; 101:455–458. [PubMed: 10850488]

Shores EW, Van Ewijk W, Singer A. Maturation of medullary thymic epithelium requires thymocytes expressing fully assembled CD3-TCR complexes. Int Immunol. 1994; 6:1393–1402. [PubMed: 7819148]

Taguchi O, Takahashi T, Seto M, Namikawa R, Matsuyama M, Nishizuka Y. Development of multiple organ-localized autoimmune diseases in nude mice after reconstitution of T cell function by rat fetal thymus graft. J Exp Med. 1986; 164:60–71. [PubMed: 3522798]

Zorn AM, Wells JM. Vertebrate endoderm development and organ formation. Annu Rev Cell Dev Biol. 2009; 25:221–251. [PubMed: 19575677]

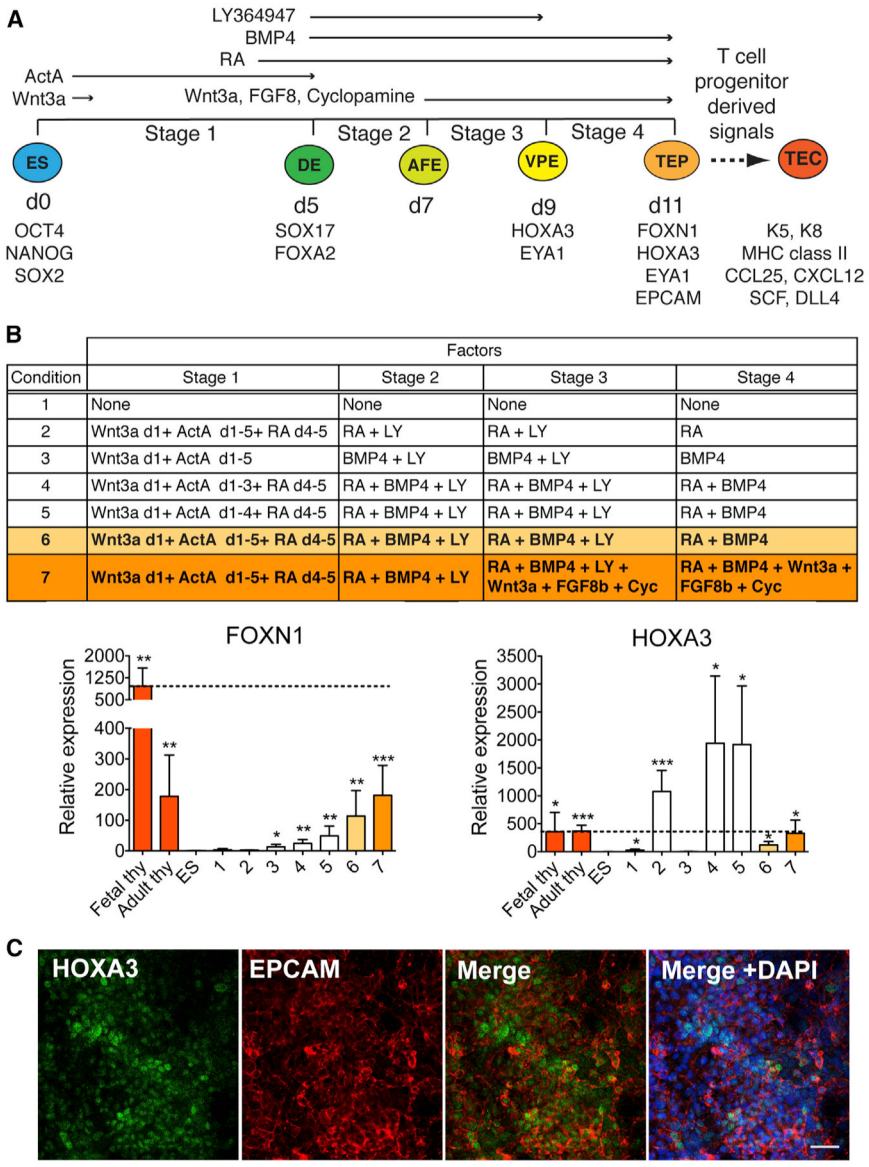

Figure 1. Directed Differentiation of hESCs into TEPs

(A) Schematic of differentiation protocol and marker genes for specific stages. ES, embryonic stem cells; DE, definitive endoderm; AFE, anterior foregut endoderm; VPE, ventral pharyngeal endoderm; TEP, thymic epithelial progenitors; TEC, thymic epithelial cells.

(B) Gene expression analysis of day 11 hESCs treated with the indicated factor combinations (conditions 1–7) (n = 4–10). Fetal and adult human thymus samples served as controls. Values are normalized to *TBP*, relative to undifferentiated hESCs, and shown as mean ± SD. Dash lines correspond to fetal expression levels that were used as a guide to optimize the differentiation protocol (*$p < 0.05$, **$p < 0.01$, ***$p < 0.001$, unpaired Student's t test, compared to undifferentiated hESCs).

(C) Immunofluorescence analysis of stage 4 cultures differentiated with condition 7 for HOXA3 (green) and EpCAM (red) protein expression. Nuclei were stained with DAPI. Scale bar = 50 μm.

See also Figure S1.

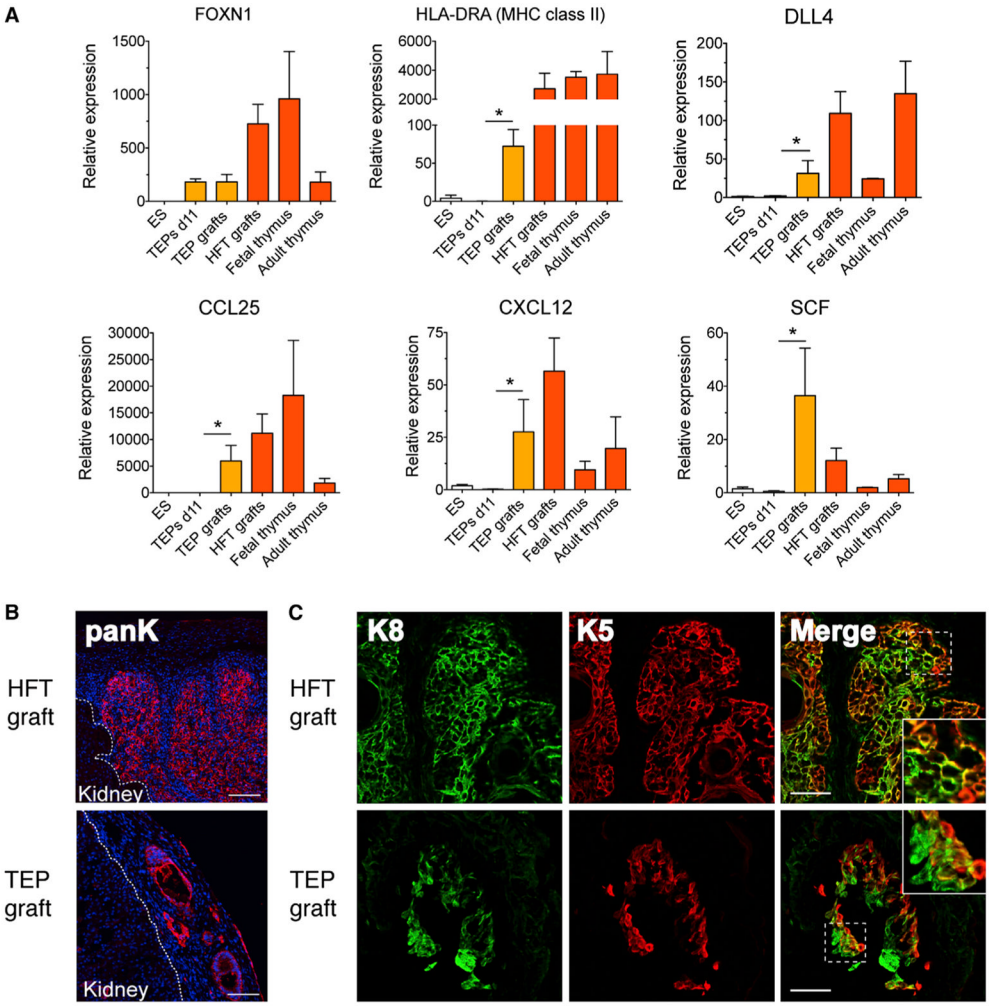

Figure 2. hESC-Derived TEPs Mature into TECs In Vivo

(A) Gene expression analysis of undifferentiated hESCs (ES, n = 4), hESCs differentiated with condition 7 (TEPs d11, n = 4), and grafts recovered from HFT (n = 5) and TEP (n = 6) recipient nude mice (8–20 weeks after transplantation). Fetal and adult human thymus samples served as controls. Values are normalized to *TBP*, relative to undifferentiated hESCs, and shown as mean ± SD (*$p < 0.05$, Mann-Whitney test, compared to TEPs d11). (B and C) Immunofluorescence analysis of HFT and TEP grafts recovered from nude mice (6–8 weeks after transplantation). (B) Epithelial cells within grafts were identified using a wide spectrum cytokeratin antibody (red). hESC-derived tissue is demarcated from the kidney by white dashed lines. Nuclei were stained with DAPI. Scale bar = 100 μm. (C) Cytokeratin 8 (K8) (green) and cytokeratin 5 (K5) (red) staining identify cortical and medullary TECs, respectively, while $K5^+/K8^+$ double positivity (yellow) indicates progenitor cells. Insets display higher magnification of dashed line areas, showing the three cell types in close proximity. Scale bar = 50 μm.

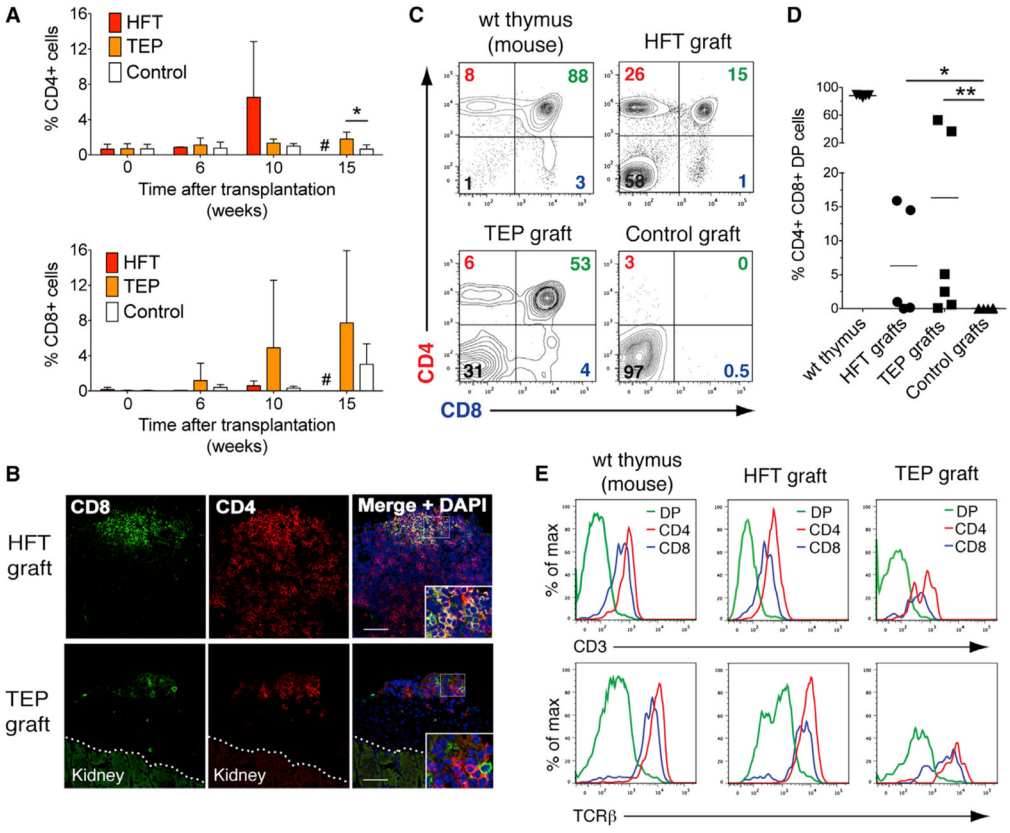

Figure 3. hESC-Derived TECs Support T Cell Development in Athymic Mice

(A) Flow cytometric analysis of cells isolated from peripheral blood of HFT (n = 2–6), TEP (n = 4–10), and control (n = 3–10) nude recipients for the presence of mouse $CD4^+$ and $CD8^+$ SP T cells. Values are shown as mean ± SD (*p < 0.05, unpaired Student's t test, compared to control); #, similar to what has been reported with other xenografts in nude animals (Taguchi et al., 1986; Fudaba et al., 2008); mice grafted with HFT started showing signs of autoimmunity and were sacrificed before 15 weeks.

(B) Immunofluorescence analysis of HFT and TEP grafts recovered from nude mice for the presence of mouse $CD8^+$ (green), $CD4^+$ (red) and $CD8^+CD4^+$ DP (yellow) T cells. hESC-derived tissue is demarcated from the kidney by white dashed lines. Nuclei were stained with DAPI. Scale bar = 50 μm.

(C–E) Flow cytometric analysis of cells recovered from WT mouse thymus, HFT, TEP, and control grafts for the presence of mouse $CD4^+$ (red), $CD8^+$ (blue) and $CD4^+CD8^+$ DP (green) T cells. (C) Representative plots from WT mouse thymus and grafts harvested 9 weeks (HFT) or 15 weeks (TEP and control) after transplantation. (D) Quantification of the percentage of mouse DP T cells in WT mouse thymus (n = 5), HFT (n = 5), TEP (n = 6), and control (n = 6) grafts harvested 4–12 weeks (HFT) or 8–22 weeks (TEP and control) after transplantation (*p < 0.05, **p < 0.01, Mann-Whitney test). (E) Cell surface expression of mouse T cell markers CD3 and TCRβ on DP T cells (green), $CD4^+$ SP T cells (red), and $CD8^+$ SP T cells (blue).

See also Figure S2.

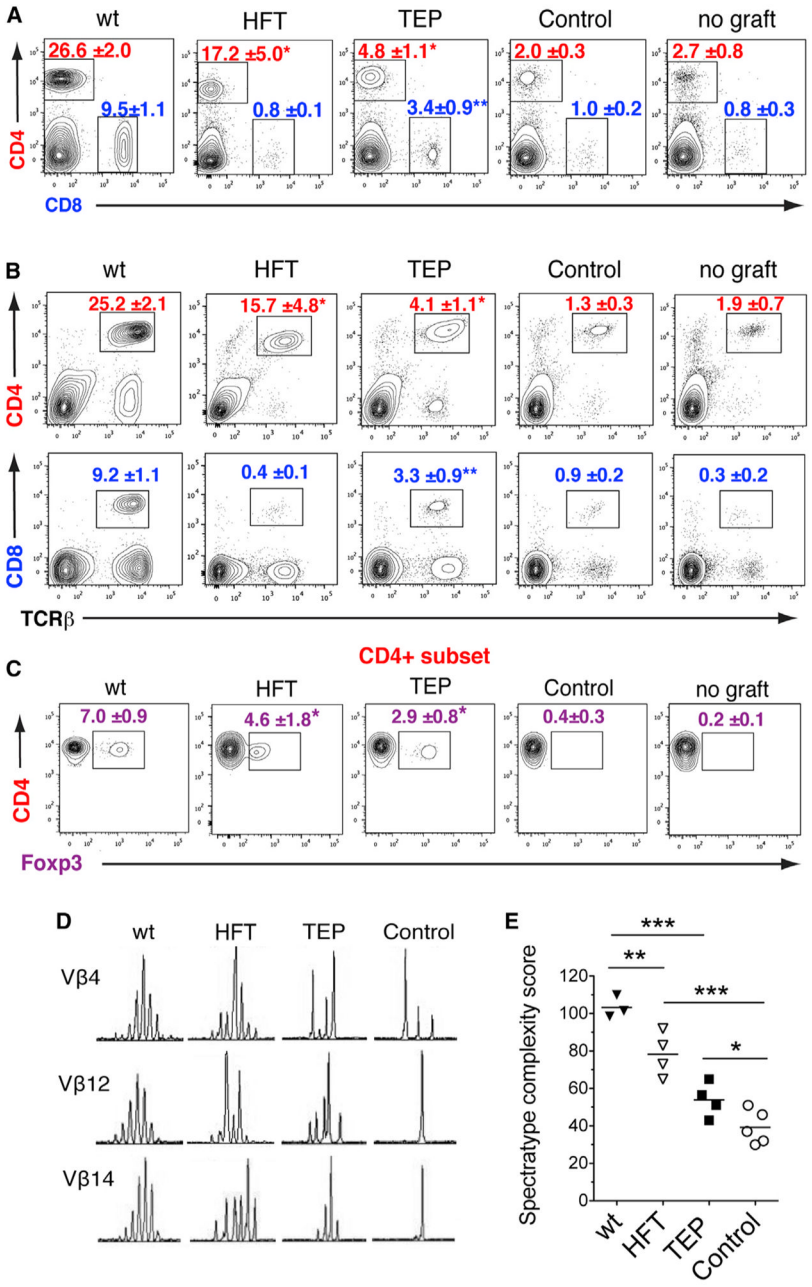

Figure 4. New T Cells Are Generated in TEP-Recipient Nude Mice

(A–C) Splenocytes recovered from WT (n = 4), HFT-grafted (n = 8), TEP-grafted (n = 4), control-grafted (n = 7), and nongrafted (n = 5) nude mice were analyzed by flow cytometry for mouse CD4, CD8, TCRβ, and Foxp3 expression. (A) Percentage of $CD4^+$ (red) and $CD8^+$ (blue) splenocytes. (B) Percentage of $CD4^+TCR\beta^+$ (red) and $CD8^+TCR\beta^+$ (blue) splenocytes. (C) Percentage of $Foxp3^+$ regulatory T cells (purple) among $CD4^+$ SP T cells. (p* < 0.05, p** < 0.01, unpaired Student's t test, compared to control.)

(D and E) Assessment of TCR repertoire diversity by spectratype analysis of the CDR3 Vβ regions of mouse T cells recovered from spleens of WT (n = 3), HFT (n = 4), TEP (n = 4), and control (n = 5) recipient nude mice. (D) Representative spec-tratypes from three Vβ families are shown. (E) Spectratype complexity score representing the sum of peaks from

each of the 24 Vβ family tested. ($p^* < 0.05$, $p^{**} < 0.01$, $^{***}p < 0.001$, unpaired Student's t test.)

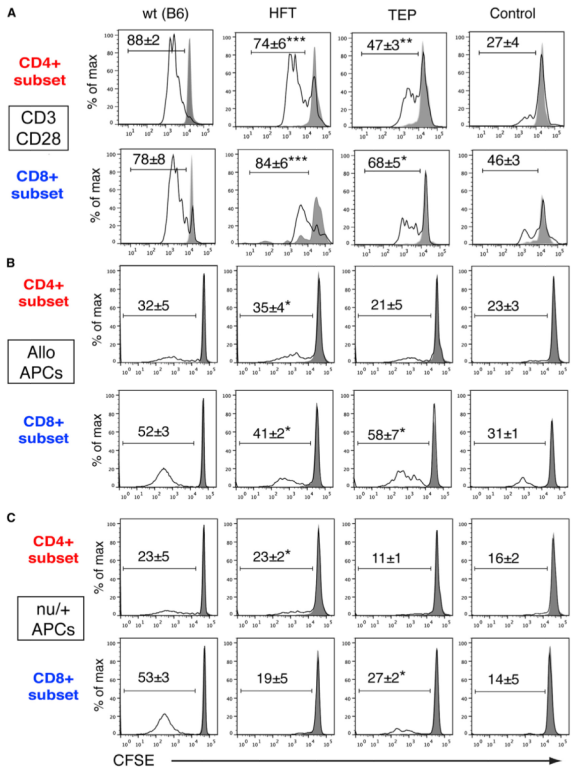

Figure 5. T Cells Generated in TEP-Recipient Nude Mice Respond To TCR and Allogeneic Stimulation In Vitro

(A) Proliferation of splenic T cells following in vitro TCR stimulation. Splenocytes from WT C57BL/6 (n = 4), HFT (n = 5), TEP (n = 4), and control (n = 6) recipient nude mice were labeled with CFSE and cultured for 3 days in the presence of anti-CD3/CD28. Cells were stained for CD4 and CD8 and gated populations were analyzed by flow cytometry for CFSE levels. Nonstimulated cells are represented by shaded histograms. (*$p < 0.05$, **$p < 0.01$, ***$p < 0.001$, unpaired Student's t test, compared to control.)

(B and C) Proliferation of enriched T cells in response to $CD11c^+$ APCs. Enriched T cells from WT C57BL/6 (n = 6–8), HFT (n = 8–10), TEP (n = 8–12), and control (n = 4–8) recipient nude mice were labeled with CFSE and cultured for 4 days in the presence of $CD11c^+$ APCs isolated from NOD (B) or nu/+ mice (C). Cells were stained for CD90.2, CD4, and CD8, and gated populations were analyzed by flow cytometry for CFSE levels. Nonstimulated cells are represented by shaded histograms. (*$p < 0.05$, unpaired Student's t test, compared to control.)

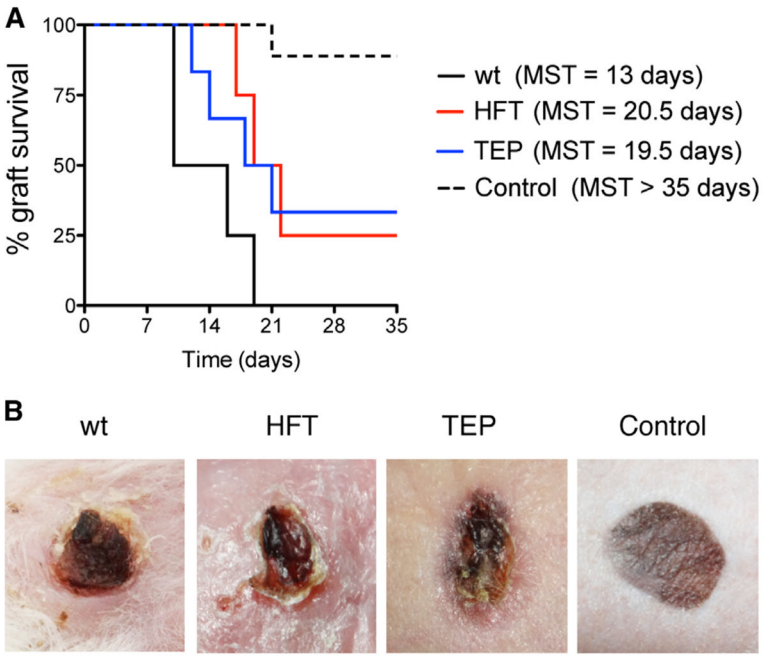

Figure 6. T Cells Generated in TEP-Recipient Nude Mice Mediate In Vivo Immune Responses

(A) Survival of allogeneic skin grafts (from C57BL/6 mice) in nu/+ (n = 4), HFT (n = 4), TEP (n = 6), and control (n = 9) recipient nude mice.

(B) Representative images of allogeneic skin grafts in nu/+, HFT, TEP, and control recipient nude mice at the time of rejection.

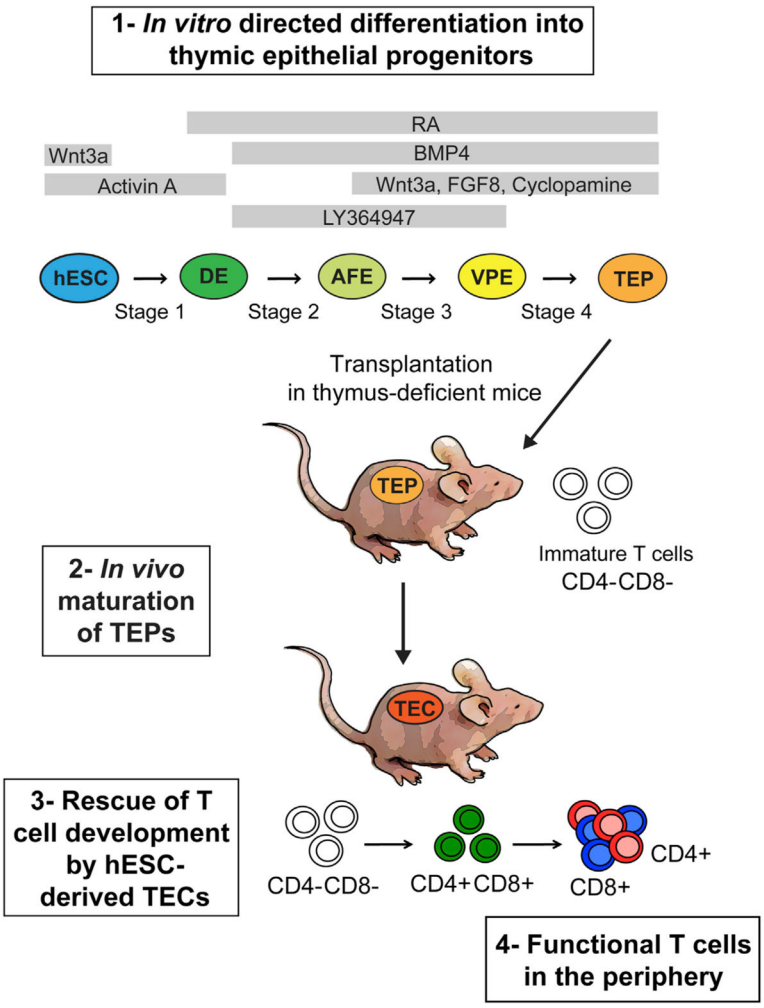

Figure 7. Model for the Generation and Maturation of hESC-Derived TEPs in Thymus-Deficient Nude Mice

(1) TEPs are generated from hESCs in vitro using the indicated combination of factors. (2) At the end of stage 4, TEPs are transplanted under the kidney capsule of thymus-deficient nude mice, which allows the in vivo maturation of TEPs into TECs. (3) In the presence of hESC-derived TECs, mouse T cell progenitors from the host can mature from $CD4^{-}CD8^{-}$ DN T cells (white) to $CD4^{+}CD8^{+}$ DP (green) and SP T cells (blue and red). (4) Functional T cells migrate to the periphery of TEP-grafted mice where they can mediate immune responses such as rejection of allogeneic skin grafts.